Medicine Insights

Article

Analyzing the Intrinsic Links and Common Therapeutic Targets between Diabetic Foot Ulcers and Liver Disease through Bioinformatics

Wenbo Li[1], Xudong Xin[1], Tianyi Shen[1], Zhenhao Zhang[1] and Jihua Wei[2,*]

[1] Youjiang Medical University for Nationalities, Baise, China
[2] Department of Sports Medicine, Affiliated Hospital of Youjiang Medical University for Nationalities, Baise, China
* Correspondence: Jihua Wei, Department of Sports Medicine, Affiliated Hospital of Youjiang Medical University for Nationalities, Baise, China

Abstract: Background. Diabetic foot ulcer (DFU) is a critical and prolonged complication of diabetes associated with high disability and mortality rates. Lipid metabolism disorders resulting from liver diseases are a key etiology in the development of diabetes mellitus and diabetic foot. Currently, there are no effective therapeutic targets or medications for treating DFU in combination with liver diseases such as nonalcoholic fatty liver disease (NAFLD)/nonalcoholic steatohepatitis (NASH) and liver cirrhosis (LC). The intrinsic links between the pathogenesis of DFU and these liver conditions have yet to be fully elucidated. Methods. We explored the molecular networks associated with DFU and NASH, as well as DFU and LC. Datasets were downloaded from the Gene Expression Omnibus (GEO) database and differentially expressed genes (DEGs) were identified. Gene Ontology (GO) and Kyoto Encyclopedia of Genes and Genomes (KEGG) enrichment analyses were performed. Protein-protein interaction (PPI) networks were constructed using the STRING database, and hub genes were identified. The co-expression framework of hub genes was analyzed, and a mRNA-miRNA-TF regulatory network was constructed. The hub genes were validated, and medication prediction and molecular docking analyses were conducted. The causal link between NAFLD and DFU was studied utilizing Mendelian randomization. Results. In DFU and NASH, 294 common DEGs were identified, with four hub genes (FOS, PTGS2, SOCS3, and CD274) associated with inflammatory, immune, and metabolic responses. In DFU and LC, 347 common DEGs were identified, with six hub genes (FOS, PTGS2, CD8A, CD44, CXCL8, and SPP1) linked to inflammatory responses, metabolic processes, and cytokine receptor interactions. Our study suggests that oxygen therapy could serve as a viable therapeutic approach for managing DFU in patients with concurrent NASH. Simvastatin, a classic lipid-lowering medication, shows potential as an effective treatment for combined with NASH or LC due to its strong binding affinity with identified hub genes. Discussion. Understanding the networks and central genes is essential for advancing our comprehension of the diverse complexities associated with diabetes and promoting the advancement of potential therapeutic strategies. Targeting these hub genes and their associated signaling pathways could provide new treatment strategies for DFU combined with NASH or LC, offering a solid theoretical foundation for future therapies.

Keywords: Diabetic foot ulcer; NAFLD; LC; bioinformatics; mendelian randomization studies; hub genes; medication prediction; immune cell infiltration

Received: 01 July 2026
Revised: 20 August 2026
Accepted: 30 August 2026
Published: 02 September 2026

1. Introduction

Diabetic foot ulcers (DFUs) are one of the most frequent and severe complications of diabetes mellitus, often resulting in circulatory and sensory disturbances in the feet. The mortality rate following the onset of DFUs is high, with a recurrence rate of 65% within 3-5 years, a lifetime lower limb amputation rate of 20%, and a 5-year mortality rate of 50%-

70% [1]. In recent years, NAFLD and its advanced form, NASH, have emerged as the most common chronic liver conditions worldwide, impacting about 25% of the population. Type II diabetes mellitus is a common cause of NAFLD/NASH, and the progression of these conditions is closely linked to the development of coronary atherosclerosis [2]. Notably, coronary atherosclerosis is a significant factor in the pathogenesis of DFUs [1]. The incidence of liver cirrhosis continues to increase annually, and lipid metabolism disorders caused by cirrhosis are a significant contributor to metabolic imbalances in diabetic patients, often leading to chronic, non-healing wounds like DFUs [3]. However, few studies have investigated the relationship between DFUs, NAFLD/NASH, and liver cirrhosis. Therefore, exploring new treatment options for DFUs in the context of liver disease holds significant scientific and clinical value.

The co-occurrence of DFU and liver disease highlights the close connection between these two complications in diabetes. Increasing evidence indicates that common pathological mechanisms, including chronic inflammation and metabolic disorders [2, 4], play a crucial role in the onset and progression of DFU, NAFLD, and cirrhosis. Exploring the shared molecular mechanisms and identifying promising therapeutic targets for DFU, NAFLD, and liver cirrhosis (LC) is critical for designing interventions that effectively tackle multiple complications associated with diabetes.

The advancement of bioinformatics offers a powerful method for discovering potential therapeutic targets shared between DFU, NAFLD, and LC [5]. Through the integration and analysis of large-scale biological datasets, bioinformatics approaches can uncover key molecules and pathways implicated in the pathogenesis of these complications [6]. Identifying common therapeutic targets is essential for developing innovative strategies to alleviate the disease burden and improve clinical outcomes and quality of life for individuals with DFU combined with NAFLD or LC.

This study seeks to investigate the shared molecular mechanisms underlying DFU, NAFLD/NASH, and LC, offering insights into the development of targeted strategies. By elucidating the common pathological processes in these conditions, the research introduces new approaches for addressing complications associated with diabetes. The research design is depicted in a flowchart (Fig 1).

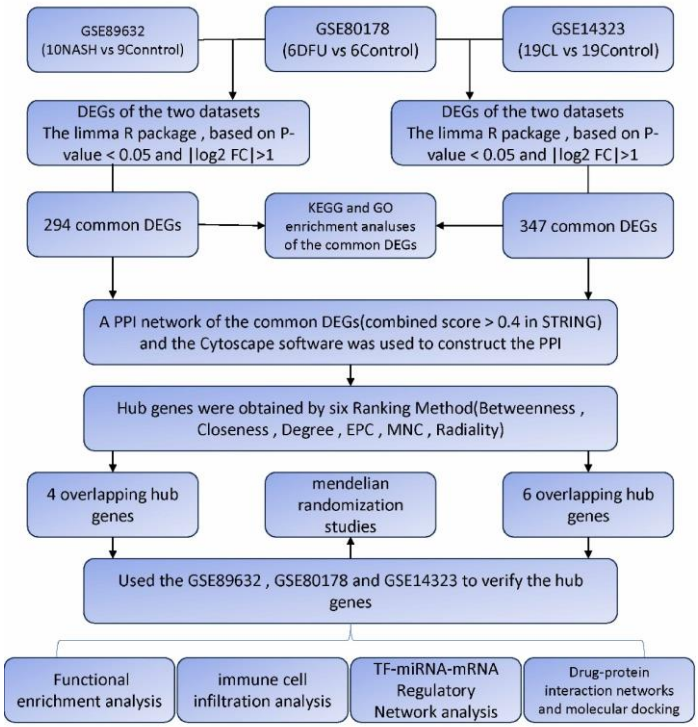

Figure 1. Flowchart of the Study Design

2. Materials & Methods

2.1. Raw Data and Downloads

The Gene Expression Omnibus (GEO, http://www.ncbi.nlm.nih.gov/geo) is publicly accessible database containing numerous high-throughput sequencing and microarray datasets from research organizations worldwide [7]. GEO was searched using the terms "NASH," "DFU," and "LC," with the inclusion criteria:(1) genome sequencing and (2) human-derived samples. Based on the GPL 16886 Affymetrix Human Gene 2.0 ST Array (Homo sapiens), the GPL 14951 Illumina HumanHT-12 WG-DASL V4.0 R2 expression beadchip (Homo sapiens), and the GPL 571 Affymetrix Human Gene 2.0 ST Array (Homo sapiens) platform, on the GPL 571 Affymetrix Human Genome U133A 2.0 Array (Homo sapiens) platform, three datasets (GSE80178, GSE89632, and GSE14323) were collected from the GEO databases for DFU, NASH, LC, and controls [8-10]. The GSE80178 dataset consists of gene expression data from 6 DFU patients and 6 healthy control samples. Similarly, the GSE89632 dataset includes data from 10 NASH patients and 9 controls, while GSE14323 provides gene expression profiles from 19 LC patients and 19 healthy controls.

2.2. Identification of Differentially Expressed Genes (DEGs)

The DEGs for DFU and NASH, as well as DFU and LC, were extracted and analyzed utilizing the Limma package in R, with a DEG screening threshold of $|\log2FC| > 1$ and an adjusted p-value of < 0.05. DEGs from the three datasets were visualized utilizing the Microbiology Letter online platform (http://www.bioinformatics.com.cn/) to generate heatmaps, volcano plots, Venn diagrams, and GO/KEGG enrichment plots. Additionally, overlapping DEGs between DFU and NASH, and DFU and LC, were identified utilizing the DAVID online platform (https://david.ncifcrf.gov/) for further analysis.

2.3. Enrichment Analysis of DEGs

The Database for Annotation, Visualization, and Integrated Discovery (DAVID) (https://david.ncifcrf.gov/) provides a comprehensive suite of functional annotation tools, enabling researchers to explore the biological significance of large gene lists. These tools are supported by the DAVID knowledge base, which integrates multiple sources of functional annotation through the DAVID Gene concept. To better understand the key biological functions of DEGs, GO and KEGG pathway analyses were performed on up- and down-regulated DEGs using DAVID. A statistically significant result was defined as an adjusted P-value of less than 0.05 [11-13].

2.4. Establishment of PPI Interaction Network and Identification of Hub Genes

The Search Tool for the Retrieval of Interacting Genes (STRING) (http: //string-db.org/) was utilized to construct PPI networks, with a minimum interaction score of >0.4 considered significant [14]. The PPI networks were visualized utilizing Cytoscape (http: www.cytoscape.org) (version 3.10.0) software [15]. A Cytoscape plug-in was employed to identify key protein expressions, and six algorithms were utilized to identify hub genes with strong connectivity within the PPI network.

2.5. Validation of Hub Gene Expression

The transcript levels of the identified hub genes were validated using datasets GSE80178 (DFU), GSE89632 (NASH), and GSE14323 (LC). A Student's t-test was employed to assess hub gene expression, with statistical significance set at a P-value < 0.05.

2.6. Immune Infiltration Analysis

The CIBERSORT algorithm was employed to examine the gene expression matrix and assess the proportions of various immune cell subpopulations within the samples. Only samples with an adjusted P-value below 0.05 were retained for further analysis. The immune cell infiltration matrix was calculated utilizing the output from the MOABS algorithm. Single-sample GSEA (ssGSEA) was conducted utilizing the "GSVA" R package, with the outcomes visualized through the "pheatmap" R package (https://CRAN.R-project.org/package=pheatmap), showing the correlation between the samples.

2.7. Transcription Factor (TF) Gene and MiRNAs Regulatory Network

TF-target interactions were retrieved through the Transcriptional Regulatory Relationships Unraveled by Sentence-based Text mining (TRRUST) (https://www.grnpedia.org/trrust/) database, which predicts transcriptional regulatory networks by identifying target genes of transcription factors and their regulatory relationships [16]. Additionally, miRNA-target interactions were obtained from the publicly available Mirwalk database (http://mirwalk.umm.uni-heidelberg.de/). Filtered miRNAs and their corresponding networks were mapped using Cytoscape [17].

2.8. Drug Evaluation and Molecular Docking Analysis

DSigDB analysis was conducted utilizing Enrichr (https://maayanlab.cloud/Enrichr/) [18]. The crystal structures of key proteins were obtained from the Protein Data Bank (https://www.rcsb.org/). Molecular docking analysis were conducted with the Autodock tool (version 1.5.7), and results were reported as binding energies. Final images were generated using the Pymol plug-in for Python 3.7.

2.9. Mendelian Randomization to Study the Causal Relationship between Nafld and DFU

A Mendelian randomization study was conducted to investigate whether NAFLD is a causal factor for DFU. Single nucleotide polymorphisms (SNPs) were used as instrumental variables (IV), with NAFLD as the exposure factor. The SNP data were obtained from the IEU OpenGWAS project (mrcieu.ac.uk). SNPs represent specific locations in the DNA sequence where single-base pair variations occur. For reliable effect estimates, IVs must meet three core assumptions: (1) relevance-the genetic variants used as IVs must be associated with the exposure; (2) independence-there must be no correlation between the IV and the outcome; and (3) exclusionary restrictions-the IV should not be linked to any confounders other than the exposure. The p-value threshold for IV was 1e-5. The LDlink (LDlink | An Interactive Web Tool for Exploring Linkage Disequilibrium in Population Groups (nih.gov)) online database was used to identify potential confounders, and the R TwoSampleMR package was applied for data analysis and visualization.

2.10. Data Availability

All data generated or analyzed during this study is included in this published article.

3. Results

3.1. Identification of DEGs

A total of 4,989 DEGs were identified in the DFU dataset, with 2,261 upregulated and 2,728 downregulated genes (Figure 2A). The NASH dataset contained 1,589 DEGs, comprising 726 upregulated and 863 downregulated genes (Figure 2A). In the LC dataset, 1,525 DEGs were detected, with 934 up-regulated and 591 down-regulated genes (Fig 2A). Venn diagram analysis revealed 294 overlapping DEGs between the DFU (GSE80178) and NASH (GSE89632) datasets, and 347 overlapping DEGs between the DFU (GSE80178) and LC (GSE14323) datasets, as shown in Figure 2B. Heatmap analysis was conducted to display the expression patterns of the overlapping DEGs in the respective datasets (GSE80178 and GSE89632; GSE80178 and GSE14323) (Fig 2C, E).

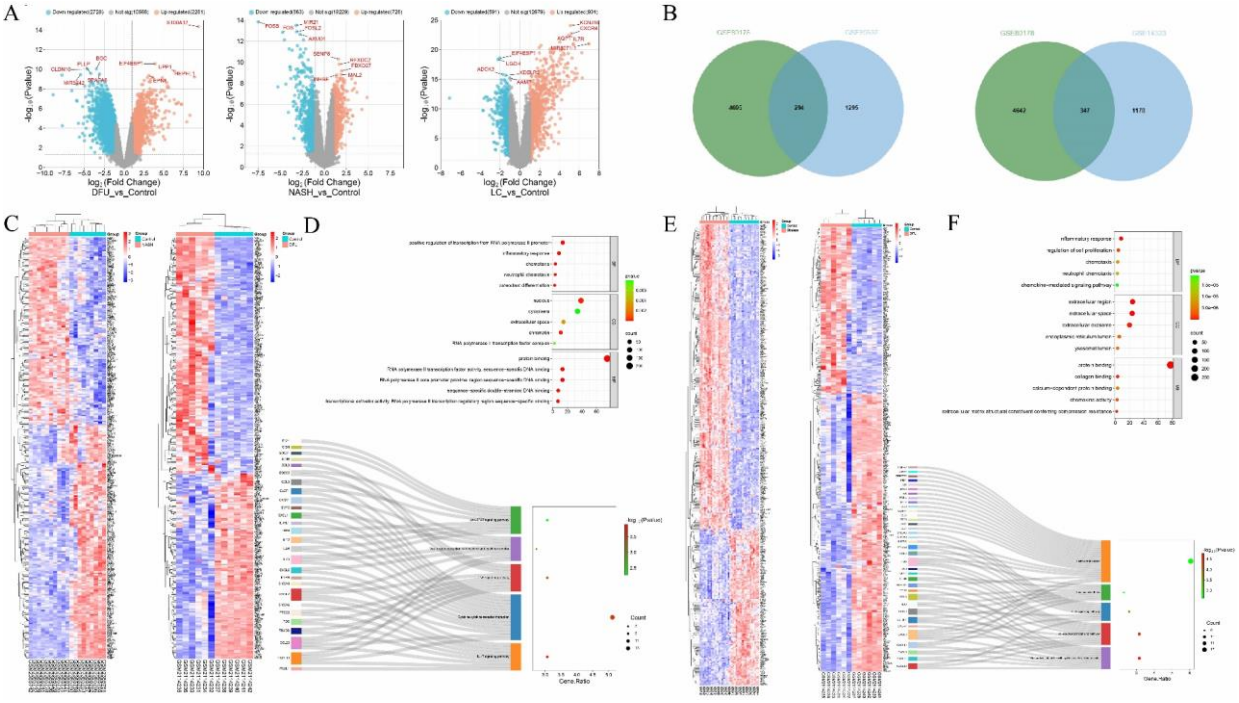

Figure 2. Volcano Plots of DEGs in the GSE80178, GSE89632, and GSE80178, GSE14323 Datasets (with Up-Regulated Genes Shown in Red and Down-Regulated Genes in Blue (a)), Venn Diagrams of Overlapping DEGs (B), and Heat Maps (C, E). Gene Ontology (GO) and Kyoto Encyclopedia of Genes and Genomes (KEGG) Enrichment Analyses of Overlapping DEGs in the GSE80178, GSE89632 (D), GSE80178(E), and GSE14323 (F) Datasets.

3.2. Enrichment Analysis of DEGs

The biological functions and the shared DEGs pathways were analyzed through GO and KEGG pathway enrichment analyses. Following threshold adjustment with a p-value < 0.05, the top five most significantly enriched GO terms and KEGG pathways were selected. Regarding biological processes, DEGs shared by DFU and NASH were mainly associated with inflammatory responses, positive transcriptional regulation of the RNA polymerase II promoter, neutrophil chemotaxis, osteoclast differentiation, and chemotaxis. Cellular composition analysis showed that DEGs were significantly enriched in the nucleus, nuclear chromatin, extracellular space, cytoplasm, and RNA polymerase II transcription factor complex. Molecular function analysis revealed enrichment in protein binding, sequence-specific DNA binding near the RNA polymerase core promoter, RNA polymerase II transcription factor activity, transcriptional activator activity, and sequence-specific double-stranded DNA binding (Figure 2D). For DFU and LC, shared DEGs were mainly involved in inflammatory responses, regulation of cell proliferation, chemotaxis, neutrophil chemotaxis, and chemokine-mediated signaling pathways. Cellular component analysis indicated significant enrichment in the extracellular matrix, extracellular space, exosomes, endoplasmic reticulum lumen, and lysosomal lumen. Molecular function analysis showed significant enrichment in protein binding, extracellular matrix structural components involved in stress resistance, collagen binding, chemokine activity, and calcium-dependent protein binding (Figure 2F). Using KEGG analysis, the top five most significant pathways in DFU and NASH were identified as IL-17 signaling, cytokine-cytokine receptor interaction, TNF signaling, viral protein-cytokine receptor interaction, and JAK-STAT signaling (Figure 2D). In DFU and LC, the top five pathways were viral protein-cytokine and cytokine receptor interaction, toll-like receptor signaling, IL-17 signaling, rheumatoid arthritis, and cancer pathways (Figure 2F).

3.3. PPI Network Construction and Hub Gene Identification

The PPI network was constructed utilizing the STRING database (Figure 3 A, B) to explore the interactions among the overlapping genes. The data were then imported into Cytoscape software for visualization and further analysis. Using the cytoHubba plug-in, six algorithms, including EPC (Figure 3, C1, D1), Closeness (Figure 3, C2, D2), Degree (Figure 3, C3, D3), MNC (Figure 3, C4, D4), Radiality (Figure 3, C5, D5), and Betweenness (Figure 3, C6, D6), were applied to calculate the top 10 hub genes for each algorithm. After comparing the results with Venn diagrams, four overlapping hub genes were identified in DFU and NASH, including FOS, PTGS2, SOCS3, and CD274, while six overlapping hub genes were found in DFU and LC, including FOS, PTGS2, CD8A, SPP1, CXCL8, and CD44.

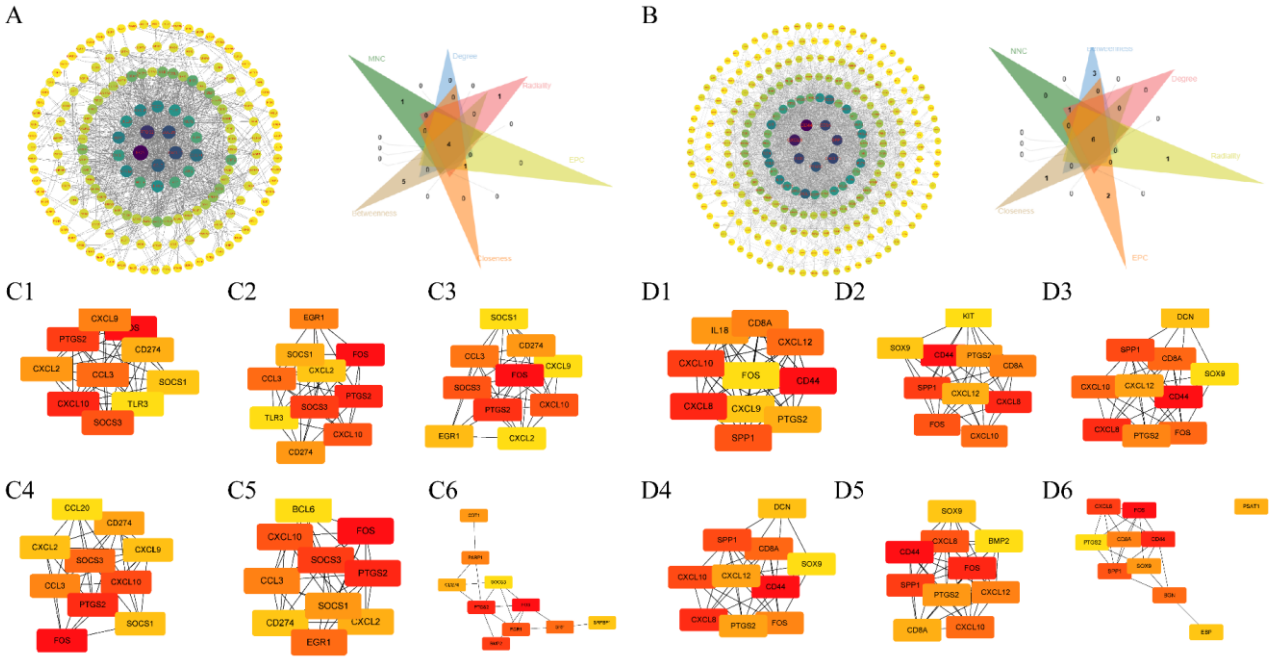

Figure 3. PPI Network Diagrams of Overlapping DEGs for DFU, NASH (a), and DFU, LC (B) Datasets and Venn Diagrams of Algorithm Results. Six Algorithms (EPC, Closeness, Degree, MNC, Radiality, and Betweenness) Were Used to Identify the Central Genes of DFU and NASH (C1-C6) and DFU and LC (D1-D6).

3.4. Expression of Hub Genes

The results demonstrated a significant upregulation of three hub genes, CD274, PTGS2, and SOCS3, in DFU (Figure 4A) and NASH (Figure 4B). Additionally, there was a significant downregulation of four hub genes, CD274, PTGS2, SOCS3, and FOS, in NASH samples compared to controls. In the comparison between DFU (Fig 4C) and LC (Fig 4D), five hub genes, FOS, PTGS2, SPP1, CXCL8, and CD8A, were markedly elevated in DCM and DFU samples compared to controls. CD44 was significantly downregulated in DFU but significantly upregulated in NASH.

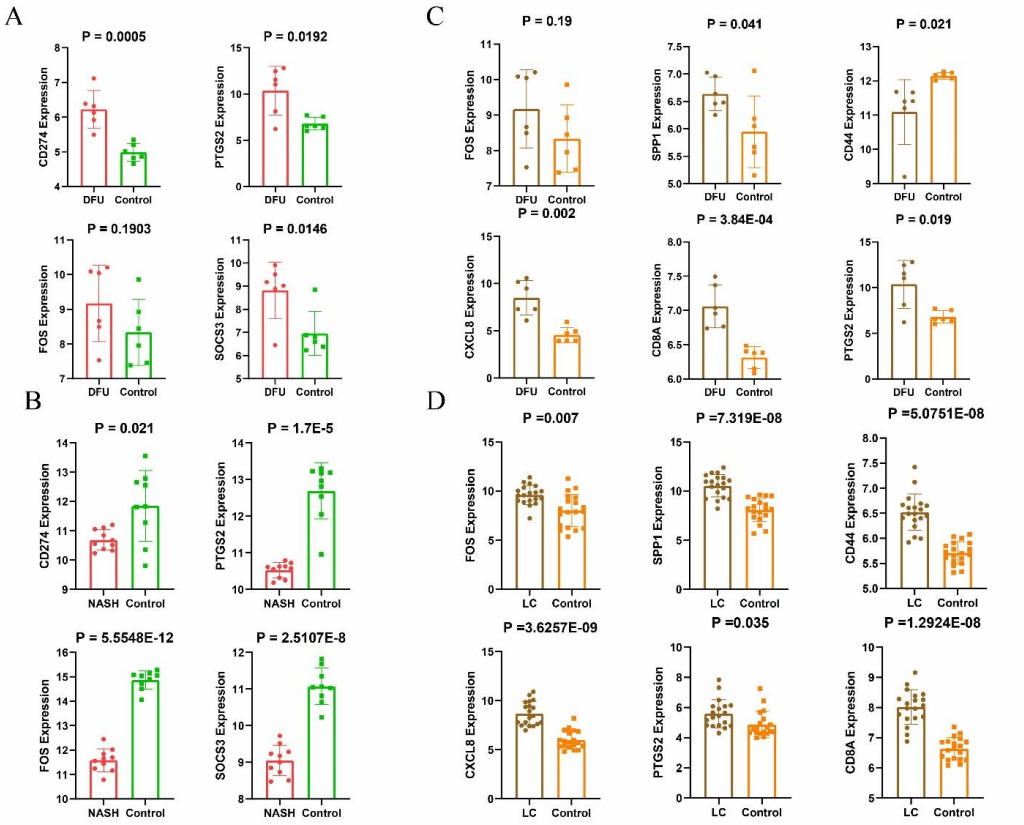

Figure 4. Expression of Hub Genes in the GEO Dataset for DFU, NASH, and LC. (A) mRNA Expression of Hub Genes in the GSE80178 Dataset (a, C). mRNA Expression of Hub Genes in the GSE89632 Dataset (B). mRNA Expression of Hub Genes in the GSE14323 Dataset (D). Data Are Expressed as the Mean.

3.5. Functional Enrichment Analysis of Proteins Interacting with Hub Genes

Functional enrichment analyses were performed on proteins interacting with the hub genes to elucidate the biological roles of each hub gene,. FOS and its interacting proteins showed significant enrichment in osteoblast differentiation and the IL-17 pathway (Figure 5A). PTGS2-related proteins were notably enriched in arachidonic acid metabolism and prostaglandin biosynthesis (Figure 5B). CD274-associated proteins were significantly enriched in cell adhesion processes and the T cell receptor pathway(Figure 5C). SOCS3 and its interacting proteins were prominently involved in the JAK-STAT signaling pathway, osteoblast differentiation, and type II diabetes mellitus (Figure 5D). CXCL8-interacting proteins were enriched in inflammatory response signaling, chemokine signaling, and cytokine-cytokine receptor interaction (Figure 5E). CD44-interacting proteins were associated with various leukocyte-related processes and cancer pathways (Figure 5F). SPP1-interacting proteins were significantly enriched in extracellular matrix-receptor interactions and PI3K-Akt signaling pathway processes (Figure 5G). CD8A-interacting proteins were enriched in immune processes, T cell receptor signaling, and antigen processing and presentation (Figure 5H). These findings highlight that hub genes are involved in a wide range of biological processes and signaling pathways, including inflammatory and immune responses, lipid metabolism, osteoclast differentiation, T cell receptor signaling, the PI3K-Akt pathway, and the JAK-STAT pathway.

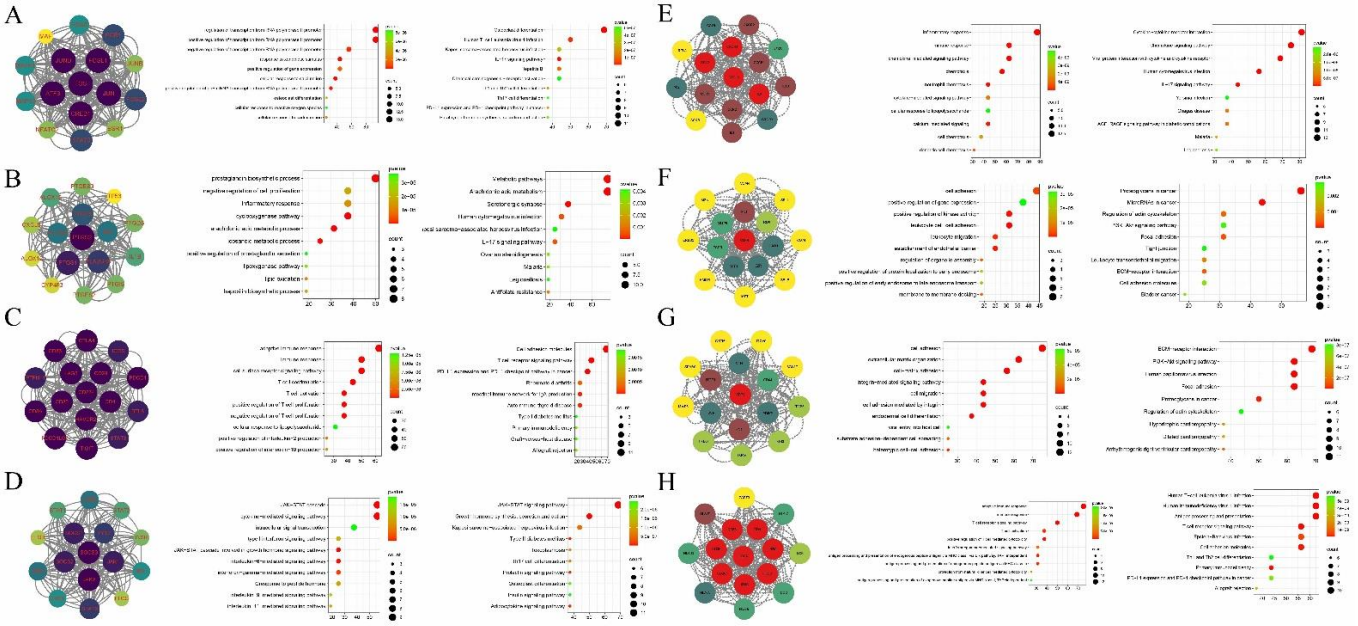

Figure 5. Functional Enrichment Analysis of Proteins Interacting with Hub Genes. A-H Protein Interaction Networks of FOS, PTGS2, CD274, SOCS3, CXCL8, CD44, SPP1, and CD8A, and BP and KEGG Analyses of Their Protein Interaction Networks, Respectively (A-H).

3.6. Differential Expression Analysis of Immune Cell Infiltration

Inflammation is a key factor in the development and progression of DFU, NASH, NASH and DFU, LC. The CIBERSORT algorithm was utilized to assess immune cell infiltration in patients with DFU, NASH, and LC, providing an evaluation of inflammation levels in these conditions. The analysis of immune cell subpopulations in DFU indicated that macrophages were the predominant infiltrating immune cells (Figure 6, A1). In NASH, the primary infiltrating immune cells were T-cell and macrophage subsets (Figure 6, A2). In LC, T-cell subsets and macrophage subsets represented the major infiltrating subpopulations (Figure 6, A3). In the hub gene mapping for DFU and NASH, hub genes showed a negative correlation with both M1 and M2 macrophages in the DFU T-cell cohort (Figure 6, B1). In the NASH T-cell cohort, SOCS3 displayed a positive link with CD4 cells, while SOCS3, FOS, and PTGS2 showed a negative correlation CD8 cells and positive correlationd with CD4 naïve T cells. In the NASH macrophage cohort, SOCS3, PTGS2, FOS, CD274, and MO-type macrophages displayed both positive and negative correlations with M1 and M2 macrophages (Figure 6, B3). In the hub gene analysis of DFU and LC, the DFU T-cell cohort showed positive correlations between SPP1, PTGS2, FOS, CXCL8, and CD8A with CD4 cells, while CD44 exhibited a negative correlation. Similarly, SPP1, PTGS2, CXCL8, and CD8A showed positive correlations with CD8 cells, whereas CD44 exhibited a negative correlation. Additionally, SPP1 and CXCL8 were negatively correlated with CD4-naïve T cells, whereas CD8A and CD44 showed a positive correlation (Figure 6, B2). In the LC T-cell cohort, SPP1, PTGS2, FOS, CXCL8, CD8A, CD44, and CD4 cells were positively correlated and negatively correlated with CD4 naïve T-cells and CD8 cells (Figure 6, B4). Correlation coefficient analysis in both DFU with NASH and DFU with LC showed significant correlations between key genes and levels of immune cell infiltration, suggesting a robust link between these conditions and immune cell presence.

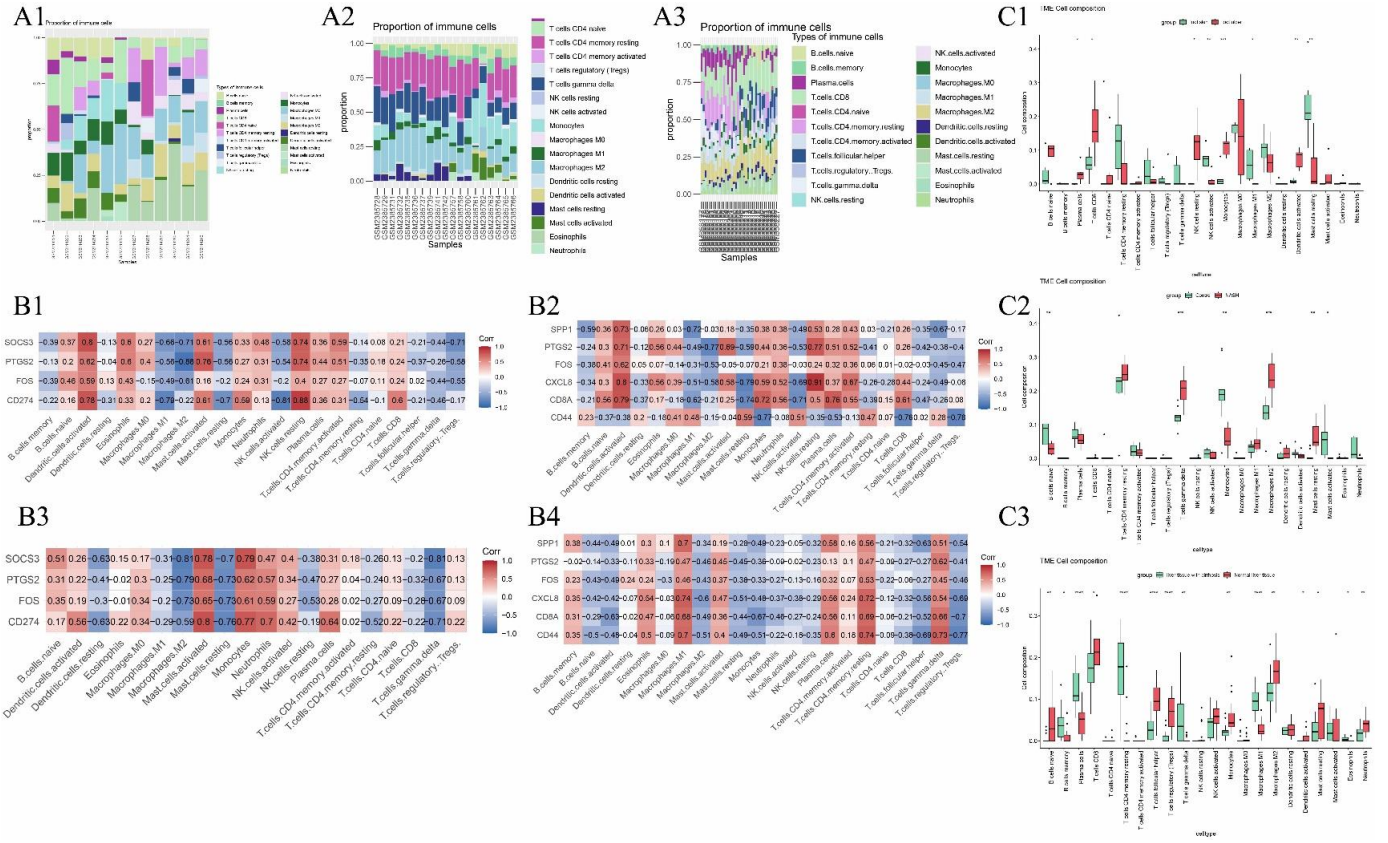

Figure 6. Immune Infiltration Analysis. A1-A3 Are the Relative Abundances of Different Immune Cell Subpopulations in DFU, NASH, and LC, Respectively (a). Correlation between Immune Cell Infiltration and Hub Gene Expression in DFU (B1, B2), NASH (B3), and LC (B4) Cohorts. C1-C3 Are the Correlations between the Expression of Immune Cell Infiltration and Hub Gene Expression in the DFU, NASH, and LC Disease Groups and the Control Group, Respectively. Box Plot (C).

3.7. Construction of Transcription Factor Genes and MiRNA Regulatory Networks

Using the TRRUST and Mirwalk databases, we identified 10 TFs and 47 miRNAs potentially regulating hub gene expression in DFU and NASH. A regulatory network was constructed by integrating 46 miRNA-mRNA pairs and 19 TF-mRNA pairs(Fig 7A). In DFU and LC, 21 TFs and 92 miRNAs were identified as potential regulators of hub gene expression, resulting in the construction of a TF-miRNA-mRNA regulatory network consisting of 93 miRNA-mRNA pairs and 51 TF-mRNA pairs (Figure 7B).

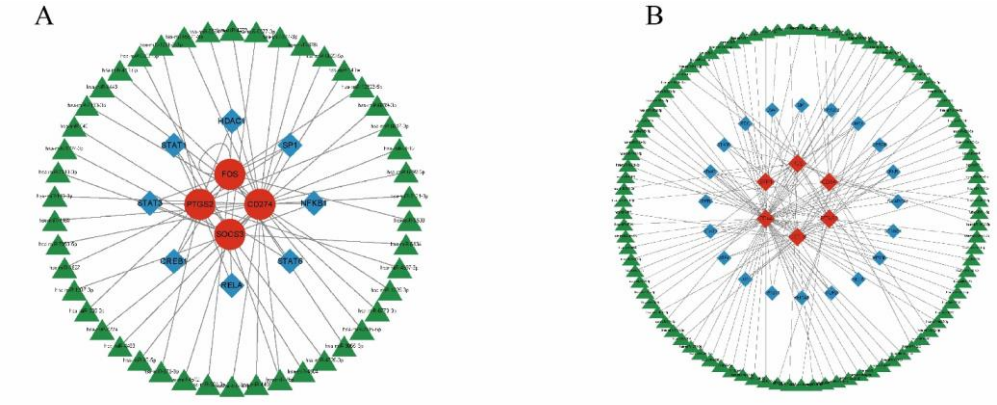

Figure 7. Construction of Transcription Factor (TF)-gene and miRNA Regulatory Networks. Validated Hub Genes for Transcription Factor and microRNA Regulatory Networks. Red: Hub Genes; Green: miRNA Genes; Blue: TF Genes. A Is DFU and NASH; B Is DFU and LC.

3.8. Identification of Drug Candidates and Targeted Chemical Interactions in DCM and DFUs

Chemical-protein interaction networks are valuable tools for elucidating protein functions and accelerating the process of drug development. Using DSigDB database enrichment, hub genes from DFU, NASH, and LC were analyzed to identify potential drug candidates. The top 10 drug candidates were chosen according to their P-values. For DFU and NASH, the top five drug candidates were oxygen, lead nitrate, benzoyl peroxide, cinnamaldehyde, and fenthion (Figure 8A). For DFU and LC, the top five candidates were benzoyl peroxide, simvastatin, mebendazole, acetaldehyde, and phorbol 12-myristate 13-acetate (Fig 8B). These drug candidates interacted with pivotal genes, suggesting their potential as treatments for both diseases.

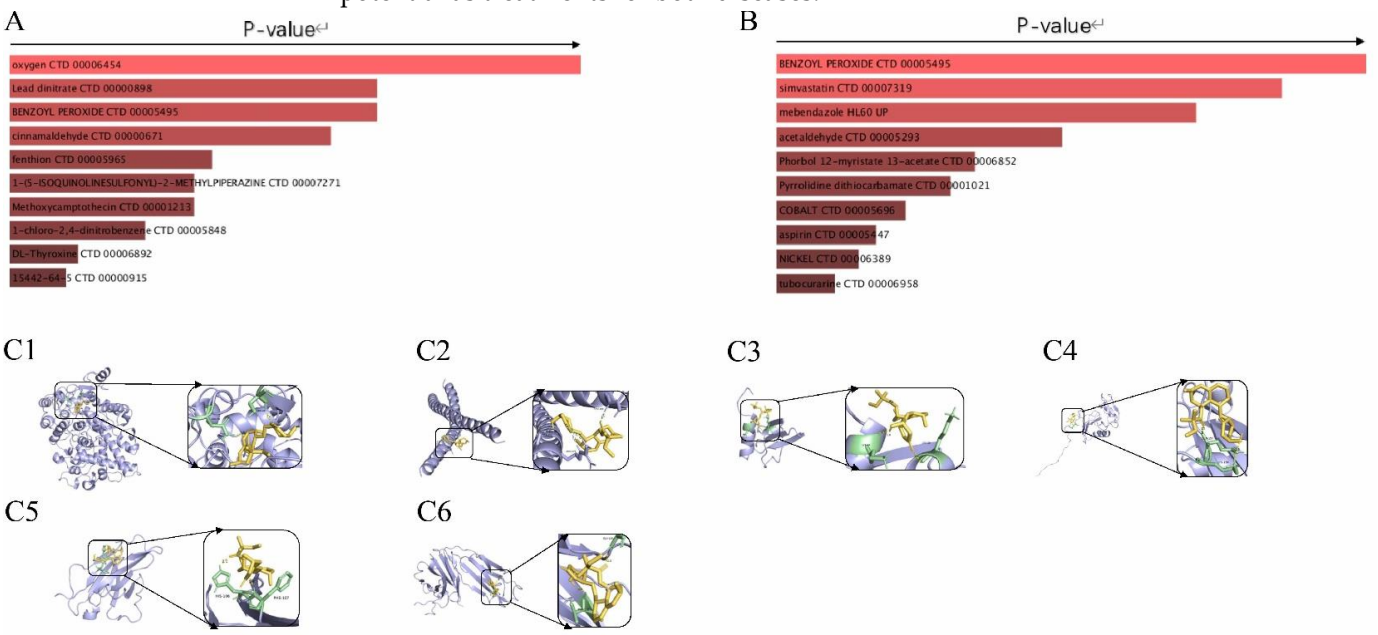

Figure 8. Identification of Drug Candidates and Molecular Docking Patterns. Combinatorial Scores of Interactions between Known Molecules and Hub Genes in the DSigDB Database (a for DFU and NASH, B for DFU and LC). Molecular Docking Patterns of Simvastatin with PTGS2 (C1), FOS (C2), CXCL8 (C3), CD44 (C4), CD8A (C5), SPP1 (C6).

Molecular docking analysis predicted the interaction between simvastatin and the hub genes PTGS2, FOS, CXCL8, CD44, CD8A, and SPP1. The molecular docking results are presented in Figures C1–C6. The results demonstrated that simvastatin exhibited low stabilization energy at the binding sites with these six target proteins, forming stable structures. AutoDock was utilized to evaluate the binding energy, as well as the number and locations of hydrogen bonds between simvastatin and the hub genes. These findings suggest that simvastatin may have therapeutic potential for treating DFU in combination with LC.

3.9. A Study of Mendelian Randomization

The results of the cull-by-cull analysis (Fig 9A), forest plot (Fig 9C), and funnel plot (Fig 9D) indicate that the contribution and stability of each SNP to the overall MR effect are satisfactory. The scatterplot (Fig 9B) demonstrates that there is a causal relationship between NAFLD and DFU. Individuals with NAFLD are more likely to suffer from DFU. Enhanced glycemic control and proper foot care are crucial for diabetic patients with nonalcoholic fatty liver disease (NAFLD). Tailoring healthcare interventions for these individuals can significantly improve the prevention and management of DFUs.

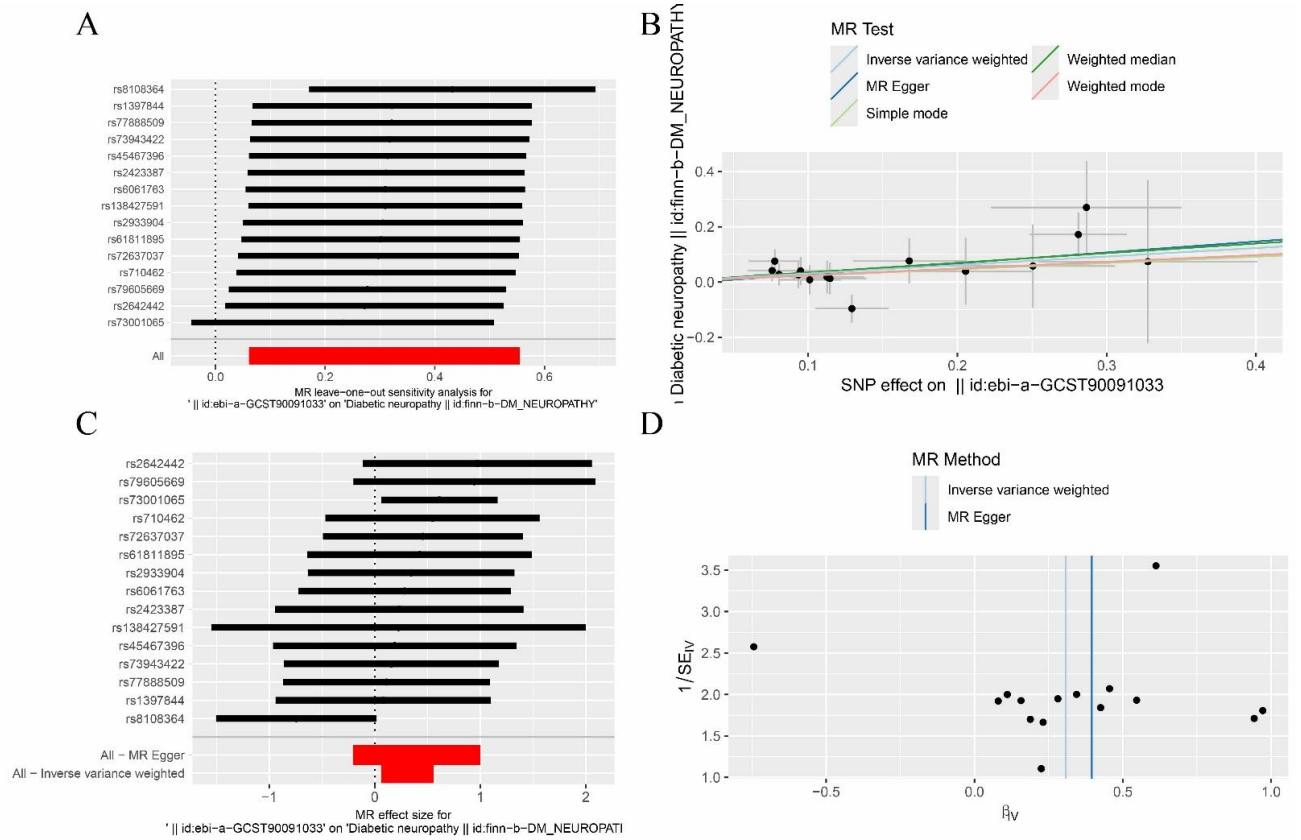

Figure 9. Mendelian Randomization Analysis, Cull-By-Cull Analysis (a); Scatterplot (B); Forest Plot (C); Funnel Plot (D)

4. Discussion

In this study, the analysis of DEGs and the development of the PPI network resulted in the identification of four hub genes (FOS, PTGS2, CD274, and SOCS3) that play crucial roles in the pathogenesis and progression of DFU and NASH . Additionally, six hub genes (FOS, PTGS2, CD8A, SPP1, CD44, and CXCL8) were highlighted for their roles in DFU and LC. Among these, PTGS2 was particularly important in DFU, NASH, and LC, suggesting a shared pathogenic mechanism between these conditions.

PTGS2, which encodes the enzyme cyclooxygenase 2 (COX-2), is known for its role in mediating inflammatory responses. COX-2 promotes the secretion of tissue factors, aggravating inflammation by activating advanced glycation end products. As COX-2 levels rise and chemotactic monocytes increase phagocytosis, the inflammatory response escalates, creating a harmful feedback loop [19]. High expression of PTGS2 typically signifies increased inflammation, particularly at DFU sites. Studies have shown that elevated PTGS2 expression in DFUs can serve as a biomarker for assessing disease severity and progression. In DFUs, retinol-binding protein (RBP) levels positively correlate with PTGS2 expression, which further correlates with the severity of the disease [19]. Additionally, the disruption of arachidonic acid (ARA) metabolism through the soluble epoxide hydrolase (sEH)/COX-2 pathway is involved in the pathogenesis of NAFLD in mice [20]. These findings are consistent with the predictions from our biological analysis.

CD274, also known as programmed death ligand 1 (PD-L1), is a co-inhibitory protein encoded by the CD274 gene in humans that plays a crucial role in regulating T cell depletion. Under normal conditions, the immune system responds to foreign antigens correlated with exogenous or endogenous danger signals, leading to the proliferation of antigen-specific CD8+ T cells and CD4+ helper cells. The binding of PD-L1 to its receptor PD-1 transmits inhibitory signals, which suppress the proliferation of antigen-specific T

cells in lymph nodes and promote apoptosis of regulatory T cells (anti-inflammatory, suppressor T cells) [21]. Previous studies have demonstrated that elevated PD-L1 levels are correlated with elevated liver enzymes and the progression of advanced liver disease [22]. In the present study, we found that T-cell subsets were more active in immune-infiltrating cells in both DFU and NASH. Therefore, reducing the inhibitory effect of CD274 on T-cells could be a critical therapeutic focus for managing DFU in combination with NASH.

SOCS3, or suppressor of cytokine signaling-3, plays a significant role in placental development, inflammation, adipose-induced weight gain, and insulin sensitivity in vivo [23]. SOCS3 primarily regulates cytokine or hormone signaling and typically acts as a preventive agent. Its main function is to bind both JAK kinase and cytokine receptors, thereby inhibiting STAT3 activation. Evidence suggests that SOCS3 regulates signaling through other STATs besides STAT3 and controls cellular pathways independent of STAT activation. It may exert its effects by directly blocking JAK activation or by mediating the ubiquitination and subsequent proteasomal degradation of cytokine, growth factor, and hormone receptors [23]. Increasing the expression of SOCS3 can ameliorate hepatic glucose-lipid metabolism disorders in type II diabetes [24]. SOCS3, identified as a hub gene, was notably reduced in NASH. This finding suggests that SOCS3 may serve as a therapeutic target to regulate hepatic glucolipid metabolism in patients with DFU combined with NASH.

CD8A, a leukocyte differentiation antigen, is a glycoprotein found on the surface of certain T cells and acts as a co-receptor for the T cell receptor (TCR). It assists the TCR in recognizing antigens and plays a role in transducing signals for T cell activation. CD8-expressing T cells (CD8+ T cells) often differentiate into cytotoxic T cells (CTLs) upon activation, enabling them to specifically kill target cells. Research has shown that CD8A levels are elevated in type II diabetes and metabolic-associated fatty liver disease (MAFLD) [25] and that CD8+ T cells are a key functional subtype positively associated with wound healing [26]. These findings suggest that CD8A may serve as a potential therapeutic target for treating DFU combined with LC.

SPP1 (secreted phosphoprotein 1), known as osteopontin, encodes a multifunctional glycoprotein that regulates extracellular matrix turnover. It plays a crucial role in osteoclast-mediated attachment to mineralized bone matrix and activates signaling pathways that modulate cell proliferation, adhesion, invasion, migration, and fibrosis through its interaction with CD44 [27]. Elevated SPP1 expression in the liver has been shown to correlate with the severity of MAFLD and hepatic T-cell markers, and it plays a critical role in initiating obesity-driven chronic inflammation by regulating T-cell accumulation and polarization [25]. Our study identified SPP1 as a crucial target gene that exhibited significant upregulation in both DFU and LC. These findings suggest that SPP1 may contribute to the advancement of DFU in combination with LC.

CD44 encodes a complex transmembrane adhesion glycoprotein expressed in a wide range of human cells, including almost all cell types in the human dermis. It plays a role in inflammatory and fibrotic processes, though its specific function in cutaneous wound healing and scarring remains largely unclear [28]. Increased CD44 expression has been linked to the onset, progression, and early signs of hepatocellular carcinoma (HCC) [29]. These findings suggest that CD44 may contribute to the development and fibrosis-related complications associated with diabetes.

CXCL8, also known as Interleukin-8 (IL-8), is a chemokine secreted by macrophages, epithelial cells, and other cell types. It is the most potent human neutrophil chemokine and exerts a chemotactic effect on neutrophils by binding to its receptors, Interleukin-8 Receptor α (IL8RA or CXCR1) and Interleukin-8 Receptor β (IL8RB or CXCR2) [30]. CXCL8 plays a critical role in regulating the inflammatory response and has been implicated in chronic trauma and cirrhosis [31,32]. These results suggest that CXCL8 may serve as a potential therapeutic target for DFU combined with LC.

We examined the immune penetration of hub genes and individual genes across our samples and found that, except CD44, the HUb genes shared a common role in M2-type

macrophage cell subsets in patients with DFU, NASH, and LC. These findings suggest that targeting the immune response of M2-type macrophage subpopulations may serve as a promising therapeutic strategy for treating DFU combined with NASH and DFU combined with LC. We used TRRUST and Mirwalk to predict the relationships between miRNAs, TF genes, and hub genes. Key regulatory targets for hub genes in DFU combined with NASH include the transcription factors STAT3, STAT6, and hsa-miR-765, offering new insights for therapeutic interventions. The key regulatory targets for DFU combined with LC may include transcription factors HDAC1, ING4, and hsa-miR-7106-3p, providing new therapeutic perspectives for these patients.

Recently, the integrated analysis of metabolomics, lipidomics, and proteomics has been extensively employed to analyze potential drug targets [33-35]. Oxygen therapy remains a key adjunctive treatment for DFU, as oxygen plays a vital role in wound healing by supporting cell proliferation, collagen synthesis, epithelial regeneration, and bacterial defense [36]. Many patients with DFU experience impaired oxygenation at the injury site, particularly when hemodynamic deficits are present. Therapeutic strategies to address this condition include local oxygen delivery to the wound and systemic oxygenation [37]. Oxygen therapy received the highest drug prediction score for patients with DFU combined with NASH, indicating it may be a preferable treatment option. Hyperbaric oxygen therapy (HBOT) is crucial in DFU treatment and can significantly enhance short-term wound healing [38]. However, the long-term benefits of HBOT remain clear, and its limitations include high cost and the ability to deliver oxygen only during therapy sessions. Therefore, a more convenient, fast, and sustainable method of delivering oxygen to DFU wounds is urgently needed.

Simvastatin is primarily used as a lipid-lowering agent indicated for the treatment of hyperlipidemia to reduce elevated total cholesterol (total-C), low-density lipoprotein cholesterol (LDL-C), apolipoprotein B (Apo B), and triglycerides (TG), and to increase high-density lipoprotein cholesterol (HDL-C). Studies have shown that hydrogels loaded with simvastatin can effectively promote angiogenesis, epithelialization, and collagen deposition and accelerate diabetic wound healing [39]. Additionally, simvastatin improves microcirculatory function in NAFLD by downregulating oxidative and ALE-RAGE stress while reducing steatosis, fibrosis, and inflammatory markers [40]. In cirrhotic disease, simvastatin inhibits the incidence of lethal bleeding, thereby reducing mortality [41]. Our study demonstrated that simvastatin interacted with key hub genes. Molecular docking analysis revealed that simvastatin forms stable hydrogen bonds with six hub genes. These findings indicate that simvastatin may serve as a promising therapeutic option for managing advanced DCM in conjunction with DFU. Overall, the results indicate that simvastatin could potentially yield considerable therapeutic benefits for individuals with diabetes mellitus and liver disease.

Mendelian randomization analysis revealed a causal relationship between NAFLD and DFU, identifying NAFLD as a significant risk factor for DFU development. For diabetic patients with NAFLD, enhanced glycemic control and diligent foot care are particularly important. Tailoring healthcare interventions for these individuals can help effectively prevent and manage DFUs.

Our review of the existing literature highlighted the lack of extensive research on shared therapeutic targets and drugs for DCM and DFU, particularly regarding bioinformatics analyses. In this study, we identified common therapeutic targets between DCM and DFU by screening overlapping DEGs, hub genes, and TFs. However, our study has some limitations. First, further validation through in vivo and in vitro experiments is required. Second, the functions of the identified hub genes need to be explored in greater detail, which will be the primary focus of our future research.

5. Conclusions

Our study offers compelling evidence that specific hub genes may significantly contribute to the shared pathogenesis of DFU and NASH, as well as DFU and LC. We identified four hub genes (FOS, PTGS2, CD274, and SOCS3) in DFU and NASH and six

hub genes (FOS, PTGS2, CD8A, and CD44) in DFU and LC. SPP1 and CXCL8 were identified as key genes, suggesting their involvement in the pathophysiology of DFU, NASH, and LC. The common hub genes FOS and PTGS2, present in DFU, NASH, and LC, may indicate an intrinsic link between these three conditions. Our findings suggest that oxygen therapy is a potential treatment for patients with DFU combined with NASH, while simvastatin, a classic lipid-lowering drug, may offer therapeutic benefits for DFU combined with LC. This study provides a foundation for exploring shared therapeutic targets and drug options for DFU with NAFLD and LC. While additional validation and exploration are required, these findings offer significant insights.

Acknowledgments: The authors thank the editors and reviewers for their valuable comments and suggestions for improving the quality of the paper and the GEO network for generously sharing the data.

Conflict of Interest: The authors declare that the research was conducted in the absence of any commercial or financial relationships that could be construed as a potential conflict of interest.

Availability of Data: The data that support the findings of this study are available in GEO at https://www.ncbi.nlm.nih.gov/geo/, reference number GSE80178, GSE89632, and GSE14323. These data were derived from the following resources available in the public domain: - GSE80178, https://www.ncbi.nlm.nih.gov/geo/query/acc.cgi?acc=GSE80178 - GSE89632, https://www.ncbi.nlm.nih.gov/geo/query/acc.cgi - GSE14323, https://www.ncbi.nlm.nih.gov/geo/query/acc.cgi

Institutional Review Board Statement: Ethics approval was not required for this research.

References

1. K. McDermott, M. Fang, A. Boulton, et al., "Etiology, epidemiology, and disparities in the burden of diabetic foot ulcers," *Diabetes Care*, vol. 46, no. 1, pp. 209–221, Jan. 2023.
2. X. Xu, K. L. Poulsen, L. Wu, et al., "Targeted therapeutics and novel signaling pathways in non-alcohol-associated fatty liver/steatohepatitis (NAFL/NASH)," *Signal Transduction and Targeted Therapy*, vol. 7, no. 1, p. 287, 2022.
3. B. Kim, E. Ban, and A. Kim, "Gelatin-alginate coacervates optimized by DOE to improve delivery of bFGF for wound healing," *Pharmaceutics*, vol. 13, no. 12, 2021.
4. X. Chen, Y. Xu, X. Meng, et al., "Analysis of the association between serum levels of 25(OH)D, retinol binding protein, and cyclooxygenase-2 and the disease severity in patients with diabetic foot ulcers," *International Wound Journal*, vol. 21, no. 3, p. e14502, Mar. 2023.
5. J. Gauthier, A. T. Vincent, S. J. Charette, et al., "A brief history of bioinformatics," *Briefings in Bioinformatics*, vol. 20, no. 6, pp. 1981–1996, Nov. 2019.
6. J. C. Navarro-Muñoz, N. Selem-Mojica, M. W. Mullowney, et al., "A computational framework to explore large-scale biosynthetic diversity," *Nature Chemical Biology*, vol. 16, no. 1, pp. 60–68, Jan. 2020.
7. R. Edgar, M. Domrachev, and A. E. Lash, "Gene Expression Omnibus: NCBI gene expression and hybridization array data repository," *Nucleic Acids Research*, vol. 30, no. 1, pp. 207–210, Jan. 2002.
8. H. A. Ramirez, I. Pastar, I. Jozic, et al., "Staphylococcus aureus triggers induction of miR-15b-5p to diminish DNA repair and deregulate inflammatory response in diabetic foot ulcers," *Journal of Investigative Dermatology*, vol. 138, no. 5, pp. 1187–1196, May 2018.
9. B. M. Arendt, E. M. Comelli, D. W. Ma, et al., "Altered hepatic gene expression in nonalcoholic fatty liver disease is associated with lower hepatic n-3 and n-6 polyunsaturated fatty acids," *Hepatology*, vol. 61, no. 5, pp. 1565–1578, May 2015.
10. V. R. Mas, D. G. Maluf, K. J. Archer, et al., "Genes involved in viral carcinogenesis and tumor initiation in hepatitis C virus-induced hepatocellular carcinoma," *Molecular Medicine*, vol. 15, no. 3–4, pp. 85–94, Mar.–Apr. 2009.
11. M. Kanehisa, M. Furumichi, Y. Sato, et al., "KEGG for taxonomy-based analysis of pathways and genomes," *Nucleic Acids Research*, vol. 51, no. D1, pp. D587–D592, Jan. 2023.
12. M. Kanehisa, "Toward understanding the origin and evolution of cellular organisms," *Protein Science*, vol. 28, no. 11, pp. 1947–1951, Nov. 2019.
13. M. Kanehisa and S. Goto, "KEGG: Kyoto Encyclopedia of Genes and Genomes," *Nucleic Acids Research*, vol. 28, no. 1, pp. 27–30, Jan. 2000.
14. A. Franceschini, D. Szklarczyk, S. Frankild, et al., "STRING v9.1: Protein–protein interaction networks, with increased coverage and integration," *Nucleic Acids Research*, vol. 41, no. Database issue, pp. D808–D815, Jan. 2013.
15. M. E. Smoot, K. Ono, J. Ruscheinski, et al., "Cytoscape 2.8: New features for data integration and network visualization," *Bioinformatics*, vol. 27, no. 3, pp. 431–432, Feb. 2011.

16. H. Han, J. W. Cho, S. Lee, et al., "TRRUST v2: An expanded reference database of human and mouse transcriptional regulatory interactions," *Nucleic Acids Research*, vol. 46, no. D1, pp. D380–D386, Jan. 2018.
17. C. Sticht, C. De La Torre, A. Parveen, et al., "miRWalk: An online resource for prediction of microRNA binding sites," *PLoS ONE*, vol. 13, no. 10, p. e0206239, Oct. 2018.
18. M. V. Kuleshov, M. R. Jones, A. D. Rouillard, et al., "Enrichr: A comprehensive gene set enrichment analysis web server 2016 update," *Nucleic Acids Research*, vol. 44, no. W1, pp. W90–W97, Jul. 2016.
19. X. Chen, Y. Xu, X. Meng, et al., "Analysis of the association between serum levels of 25(OH)D, retinol binding protein, and cyclooxygenase-2 and the disease severity in patients with diabetic foot ulcers," *International Wound Journal*, vol. 21, no. 3, p. e14502, Mar. 2023.
20. C. Y. Zhang, X. H. Tan, H. H. Yang, et al., "COX-2/sEH dual inhibitor alleviates hepatocyte senescence in NAFLD mice by restoring autophagy through Sirt1/PI3K/AKT/mTOR," *International Journal of Molecular Sciences*, vol. 23, no. 15, 2022.
21. J. H. Cha, L. C. Chan, C. W. Li, et al., "Mechanisms controlling PD-L1 expression in cancer," *Molecular Cell*, vol. 76, no. 3, pp. 359–370, Nov. 2019.
22. L. A. Orci, M. Kreutzfeldt, N. Gossens, et al., "Tolerogenic properties of liver macrophages in non-alcoholic steatohepatitis," *Liver International*, vol. 40, no. 3, pp. 609–621, Mar. 2020.
23. B. Carow and M. E. Rottenberg, "SOCS3, a major regulator of infection and inflammation," *Frontiers in Immunology*, vol. 5, p. 58, 2014.
24. L. Xu, Y. Li, L. Yin, et al., "miR-125a-5p ameliorates hepatic glycolipid metabolism disorder in type 2 diabetes mellitus through targeting of STAT3," *Theranostics*, vol. 8, no. 20, pp. 5593–5609, 2018.
25. F. Soysouvanh, D. Rousseau, S. Bonnafous, et al., "Osteopontin-driven T-cell accumulation and function in adipose tissue and liver promoted insulin resistance and MAFLD," *Obesity*, vol. 31, no. 10, pp. 2568–2582, Oct. 2023.
26. L. Guo, Z. Zhu, C. Shi, et al., "Drug suspending during wound healing effectively weakens immunosuppression-related complications by preserving CD8(+) T cell function," *Wound Repair and Regeneration*, vol. 31, no. 4, pp. 489–499, Jul./Aug. 2023.
27. Z. Song, W. Chen, D. Athavale, et al., "Osteopontin takes center stage in chronic liver disease," *Hepatology*, vol. 73, no. 4, pp. 1594–1608, Apr. 2021.
28. P. Govindaraju, L. Todd, S. Shetye, et al., "CD44-dependent inflammation, fibrogenesis, and collagenolysis regulates extracellular matrix remodeling and tensile strength during cutaneous wound healing," *Matrix Biology*, vol. 75–76, pp. 314–330, Mar. 2019.
29. S. Mustika, H. Wijaya, and B. Pratomo, "The expressions of CD44, CD90 and alpha fetoprotein biomarkers in Indonesian patients with advanced liver disease: An observational study," *Acta Medica Indonesiana*, vol. 51, no. 2, pp. 137–144, Apr. 2019.
30. S. Cambier, M. Gouwy, and P. Proost, "The chemokines CXCL8 and CXCL12: Molecular and functional properties, role in disease and efforts towards pharmacological intervention," *Cellular & Molecular Immunology*, vol. 20, no. 3, pp. 217–251, Mar. 2023.
31. M. S. Agren, T. Litman, J. O. Erikksen, et al., "Gene expression linked to reepithelialization of human skin wounds," *International Journal of Molecular Sciences*, vol. 23, no. 24, 2022.
32. M. M. Langer, S. Sichelschmidt, A. Bauschen, et al., "Pathological neutrophil migration predicts adverse outcomes in hospitalized patients with liver cirrhosis," *Liver International*, vol. 43, no. 4, pp. 896–905, Apr. 2023.
33. L. Scisciola, U. Chianese, V. Caponigro, et al., "Multi-omics analysis reveals attenuation of cellular stress by empagliflozin in high glucose-treated human cardiomyocytes," *Journal of Translational Medicine*, vol. 21, no. 1, p. 1–662, 2023.
34. Y. Xi, D. Chen, Z. Dong, et al., "Multi-omics insights into potential mechanism of SGLT2 inhibitors cardiovascular benefit in diabetic cardiomyopathy," *Frontiers in Cardiovascular Medicine*, vol. 9, p. 999254, 2022.
35. Y. Zhang, Z. Zhang, C. Li, et al., "Metabolomics study reveals the alteration of fatty acid oxidation in the hearts of diabetic mice by empagliflozin," *Molecular Omics*, vol. 18, no. 7, pp. 643–651, Jul. 2022.
36. G. De Smet, L. F. Kroese, A. G. Menon, et al., "Oxygen therapies and their effects on wound healing," *Wound Repair and Regeneration*, vol. 25, no. 4, pp. 591–608, Jul./Aug. 2017.
37. E. Everett and N. Mathioudakis, "Update on management of diabetic foot ulcers," *Annals of the New York Academy of Sciences*, vol. 1411, no. 1, pp. 153–165, Jan. 2018.
38. R. J. Goldman, "Hyperbaric oxygen therapy for wound healing and limb salvage: A systematic review," *PM&R*, vol. 1, no. 5, pp. 471–489, May 2009.
39. M. Rezvanian, S. F. Ng, T. Alavi, et al., "In-vivo evaluation of alginate-pectin hydrogel film loaded with simvastatin for diabetic wound healing in streptozotocin-induced diabetic rats," *International Journal of Biological Macromolecules*, vol. 171, pp. 308–319, Mar. 2021.
40. E. Pereira, B. P. Araujo, K. L. Rodrigues, et al., "Simvastatin improves microcirculatory function in nonalcoholic fatty liver disease and downregulates oxidative and ALE-RAGE stress," *Nutrients*, vol. 14, no. 3, 2022.
41. H. Zhang, Q. Zhang, S. Li, et al., "Simvastatin is efficacious in treating cirrhosis: A meta-analysis," *Journal of Clinical Gastroenterology*, vol. 56, no. 8, pp. e303–e312, Aug. 2022.